small, a perfectly sinusoidal surface emerges whereas it does not when the difference is large. Regardless of the type, however, the period of the self-assembled structure is the same as that of the mold pattern. The intrinsic buckling wavelength of the thin bilayer cannot be predicted by the conventional approach. We have derived a relationship for the intrinsic wavelength based on free energy minimization and found it to describe experimental results quite well even though it does not have any fitting parameters.

Experimental

For the physical self-assembly by anisotropic buckling, we used PDMS (Sylgard 184, Dow Corning) as the elastomer and fabricated PDMS molds with patterns by casting PDMS against complementary relief structures prepared by photolithography. For the polymer, we used commercial PS (molecular weight = 2.3×10^5) for the polymer and silicon wafer (100) as the substrate. Polymer films were spin-coated onto the substrate to various thicknesses ranging from 150 nm to 800 nm and the aluminum was deposited onto the polymer surface, ranging in thickness from 30 nm to 100 nm, by thermal evaporation. A patterned PDMS mold was then placed on the metal surface. A spontaneous conformal contact is realized due to the good wetting property of PDMS mold with the metal. The bilayer was then heated to a temperature above the glass transition (T_g) of the polymer for hours, typically two hours. The annealing temperature was varied between 110 °C and 130 °C. However, the experiments were carried out primarily at 120 °C due to too small an amplitude at 110 °C (< 10 nm) and due to film breakage occurring at 130 °C.

With the PDMS mold making conformal contact with the metal, anisotropic buckling resulted, unlike the isotropic buckling shown in Figure 3, because of the strong wetting of the PDMS pattern with the metal surface due to strong interactions between the two hydrophobic surfaces. As such, the buckling wave has its peak points in the void regions of the mold that are not in contact with the metal surface. Therefore, sinusoidal buckling patterns form that are a negative replica of the PDMS pattern. After cooling to ambient temperature, the mold was removed and the resulting structures were examined by atomic force microscopy (AFM).

Received: April 25, 2002

[1] J. Aizenberg, A. J. Black, G. M. Whitesides, *Nature* **1999**, *398*, 495.
[2] D. Wang, S. G. Thomas, K. L. Wang, Y. Xia, G. M. Whitesides, *Appl. Phys. Lett.* **1997**, *70*, 1593.
[3] Y. Xia, G. M. Whitesides, *Angew. Chem. Int. Ed.* **1998**, *37*, 551.
[4] D. H. Gracias, V. Kavthekar, J. C. Love, K. E. Paul, G. M. Whitesides, *Adv. Mater.* **2002**, *14*, 235.
[5] K. Y. Suh, H. H. Lee, *Adv. Mater.* **2002**, *14*, 346.
[6] G. Reiter, *Phys. Rev. Lett.* **1992**, *68*, 75.
[7] K. Y. Suh, J. Park, H. H. Lee, *J. Chem. Phys.* **2002**, *116*, 7714.
[8] H. G. Allen, *Analysis and Design of Structural Sandwich Panels*, Pergamon, New York **1969**.
[9] S. P. Timoshenko, J. M. Gere, *Theory of Elastic Stability*, McGraw Hill, New York **1961**.
[10] N. Bowden, S. Brittain, A. G. Evans, J. W. Hutchinson, G. M. Whitesides, *Nature* **1998**, *393*, 146.
[11] W. T. S. Huck, N. Bowden, P. Onck, T. Pardoen, J. W. Hutchinson, G. M. Whitesides, *Langmuir* **2000**, *16*, 3497.
[12] K. Y. Suh, Y. S. Kim, H. H. Lee, *Adv. Mater.* **2001**, *13*, 1386.
[13] W. W. Mullins, *J. Appl. Phys.* **1959**, *30*, 77.
[14] N. Sridhar, D. J. Srolovitz, Z. Suo, *Appl. Phys. Lett.* **2001**, *78*, 2482.
[15] R. Huang, Z. Suo, *J. Appl. Phys.* **2002**, *91*, 1135.
[16] K. Dalnoki-Veress, B. G. Nickel, J. R. Dutcher, *Phys. Rev. Lett.* **1999**, *82*, 1486.
[17] G. H. Fredrickson, A. Ajdari, L. Leibler, J. Carton, *Macromolecules* **1992**, *25*, 2882.
[18] J. Wang, M. Tolan, O. H. Seeck, S. K. Sinha, O. Bahr, M. H. Rafailovich, J. Sokolov, *Phys. Rev. Lett.* **1999**, *83*, 564.
[19] J. Groenwold, *Physica A* **2001**, *298*, 32.
[20] J. Kim, H. H. Lee, *J. Polym. Sci. Polym. Phys.* **2001**, *39*, 1122.
[21] J. D. Ferry, *Viscoelastic Properties of Polymers*, John Wiley & Sons, New York **1980**.

Fabrication and Properties of Composites of Poly(ethylene oxide) and Functionalized Carbon Nanotubes**

By *Huaizhi Geng*, *Rachel Rosen*, *Bo Zheng*, *Hideo Shimoda*, *Leslie Fleming*, *Jie Liu*, and *Otto Zhou**

Carbon nanotubes (CNTs)[1,2] have dimensions similar to those of typical polymeric chains, with 1–50 nm in diameter and 1–10 μm in length. Experimental results on *individual* carbon nanotubes and nanotube bundles show that they have exceptional electrical and mechanical properties with an elastic modulus of ~1 TPa and fracture strain of 5–10 %.[3] The thermal conductivity of the nanotubes is expected to be higher than that of the carbon fibers because of their structural perfection. As a result there are considerable interests in utilization of CNTs as fillers for thermal management and structural reinforcement. Although there are several published studies on polymer CNT composites,[4–9] realization of the expected enhancement in properties, especially mechanical properties, has by and large not been demonstrated. This is in part because of the difficulties in materials processing arising from insolubility of the pristine CNTs.

Recent studies have shown that CNTs can be chemically functionalized such that they are soluble in selected solvents.[10,11] Mickelson et al. reported that fluorinated single-walled carbon nanotubes (SWNTs; F-SWNTs) were dissolved in 2-propanol at a concentration of 1 mg/mL at room temperature (RT).[12] The nanotubes appear to be intact and are electrically insulating after fluorination. The enhanced solubility and potential of tailoring the interfacial bonding between the nanotubes and the matrix by modifying the side-groups make functionalized CNTs attractive fillers for composites. Here, we report results from initial studies of composites of F-SWNTs and a semi-crystalline thermoplastic polymer, poly(ethylene oxide) (PEO). Electron microscopy and thermal analysis showed that they have improved uniformity and nanotube dispersion compared with those by pristine SWNTs. Significant enhancement of the mechanical properties was obtained. The storage modulus (E') and yield strength increased

[*] Prof. O. Zhou, H. Z. Geng
Curriculum in Applied and Materials Sciences
University of North Carolina at Chapel Hill
Chapel Hill, NC 27599 (USA)
E-mail: zhou@physics.unc.edu
Prof. O. Zhou, R. Rosen, Dr. H. Shimoda, L. Fleming
Department of Physics and Astronomy
University of North Carolina at Chapel Hill
Chapel Hill, NC 27599 (USA)
B. Zheng, Prof. J. Liu
Department of Chemistry
Duke University
Durham, NC 27708 (USA)

[**] This work was supported by a grant from NASA (NAG-1-01061) and the Office of Naval Research under a MURI grant at UNC (N00014-98-1-0597). H. Z. Geng was supported by a Merit Scholarship from UNC. We thank E. Samulski for suggesting the roll-cast method and E. L. Thomas for helpful discussions.

  0935-9648/02/1910-1387 $ 17.50+.50/0

ADVANCED MATERIALS

monotonically with increasing F-SWNT loading. At 4 wt.-% loading, the RT E' is 400 % of that of the control sample. Further analysis indicates strong interfacial bonding between the F-SWNTs and the PEO matrix.

SWNT bundles[13] were synthesized by the laser-ablation method under conditions described elsewhere.[14] The raw materials were purified to remove the impurity phases such as amorphous carbon and graphitic nanoparticles by reflux in H_2O_2 followed by filtration.[15] Transmission electron microscopy (TEM) and X-ray diffraction studies show that the samples contain over 90 % SWNT bundles with the average bundle diameter of 30–50 nm, tube diameter of 1.4 nm, and bundle length of 5–10 μm. The purified SWNTs were fluorinated using the conditions described before (see Experimental).[12] Figure 1 shows a representative TEM image of the fluorinated SWNTs.

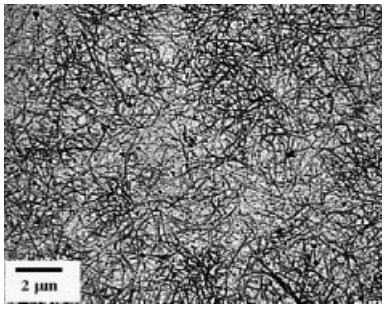

Fig. 1. TEM image of fluorinated SWNTs. Compared with as-purified materials, the diameters of the fluorinated SWNT bundles are smaller (~10 nm instead of 30–50 nm) and they disperse better in the solvent. The low image contrast is related to the small bundle size.

PEO/SWNT composite membranes with F-SWNT loading of 1, 4, 6, and 10 wt.-% and control samples (pure PEO) were prepared under the same conditions by roll-casting[16] (see Experimental).

To examine the dispersion of the nanotubes, samples were microtomed into membranes ~90 nm in thickness and were studied by TEM. Within the limited view of high-resolution TEM, no conglomeration of the F-SWNTs was observed. The nanotube bundles did not show any preferred orientation in the polymer matrix. Differential scanning calorimetry (DSC) measurements were performed using a Perkin-Elmer Pyris 1 DSC system. The results obtained in the first heating cycle are shown in Figure 2. For the control sample, an endothermic peak centered at 72.0 °C was observed upon heating. This is attributed to melting of the crystalline phase of the semi-crystalline PEO. The measured latent heat, which reflects the amount of crystalline phase in the sample, is 135.3 J/g (normalized by the total weight of the semi-crystalline sample). Both the melting temperature and the latent heat are consistent with the values reported in the literature.[17] For composites with F-SWNT loading ≤ 6 wt.-%, a single endothermic peak was observed with a slightly lower melting temperature of 66–65 °C. The sample with 10 wt.-% of F-SWNT showed two endothermic peaks centered at 72.3 °C, the melting temperature of pure crystalline PEO phase, and 65 °C, respectively. These results indicate that single-phase F-SWNT/PEO blend was formed at ≤ 6 wt.-% F-SWNT loading, while phase separation (into regions of pure PEO and regions of PEO/F-SWNT) occurred at higher F-SWNT loading due to conglomeration of F-SWNTs. No significant change in the crystallinity of the PEO matrix was observed. The measured latent heats are 135.3 J/g, 118.7 J/g, and 146.6 J/g for the control sample (pure PEO), and PEO blended with 1 and 4 wt.-% of F-SWNTs, respectively.

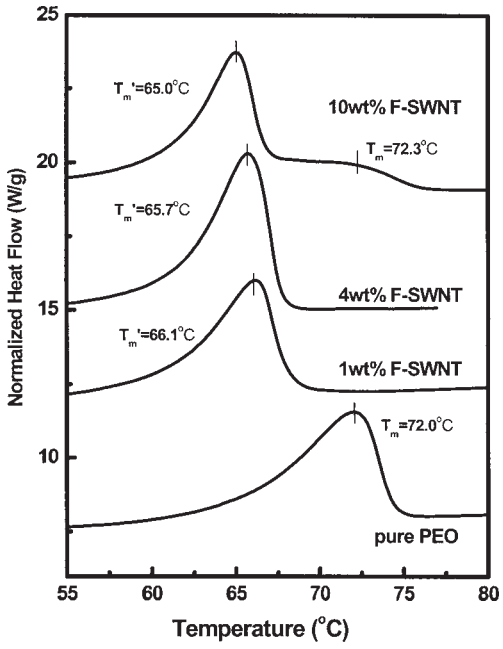

Fig. 2. Differential scanning calorimetry (DSC) data of pure PEO and PEO/F-SWNT composites. The endothermic peak on the heating curve is attributed to melting of the crystalline phase of the PEO matrix. The melting temperature is 72 °C for the control sample with a latent heat of 135.3 J/g. The temperature is reduced to ~65 °C for the composites. The re-appearance of a second endothermic peak at ~72 °C in the 10 wt.-% F-SWNT composite indicates macroscopic phase separation into regions of pure PEO and regions of PEO/F-SWNTs.

The mechanical properties were investigated using a dynamic mechanical analyzer system (Perkin-Elmer DMA7e) using either the oscillatory mode (1 Hz) or the tensile stress–strain mode in the temperature range of –150 °C to 60 °C. For dynamic measurements, a sinusoidal force with a frequency of 1 Hz and amplitude of 60 mN was applied to the sample. By analysis of the corresponding strain, the storage modulus (E') and loss modulus (E'') were obtained. In the tensile test, the load was increased at a rate of 100 mN/min. For each F-SWNT concentration, several samples were measured under the same conditions. Figure 3 shows the storage modules of one set of samples obtained in the first cooling and heating cycle. The 20 °C E's from all the samples measured are plotted in Figure 3 inset as E' versus wt.-% of F-SWNT loading. The storage moduli of the composites are significantly higher than that of the pure PEO in the entire temperature range of the experiment, and increased monotonically with increasing F-SWNT loading. As shown in Figure 3, inset, the averaged 20 °C E' (over several samples with the same F-SWNT concentration) increased from 0.3 GPa for pure PEO to 1.2 GPa

  0935-9648/02/1910-1388 $ 17.50+.50/0

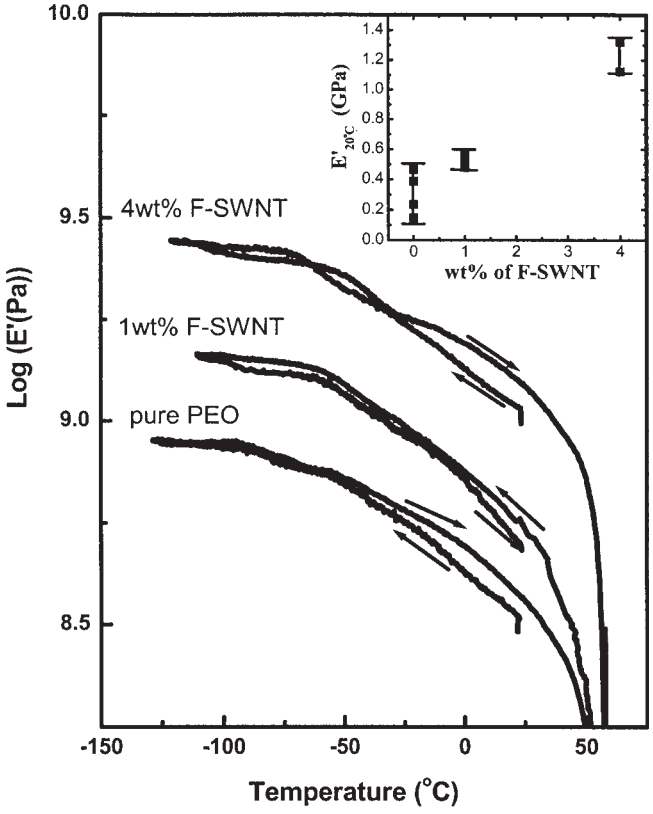

Fig. 3. The storage modulus (E') of the F-SWNT composites measured using a dynamics mechanical analyzer at 1 Hz. The inset shows the room-temperature E' values versus wt.-% of F-SWNT loading from all the samples measured under the same conditions. The averaged 20 °C E' (over several samples with the same F-SWNT concentration) increased from 0.3 GPa for pure PEO to 1.2 GPa for PEO blended with 4 wt.-% of F-SWNT.

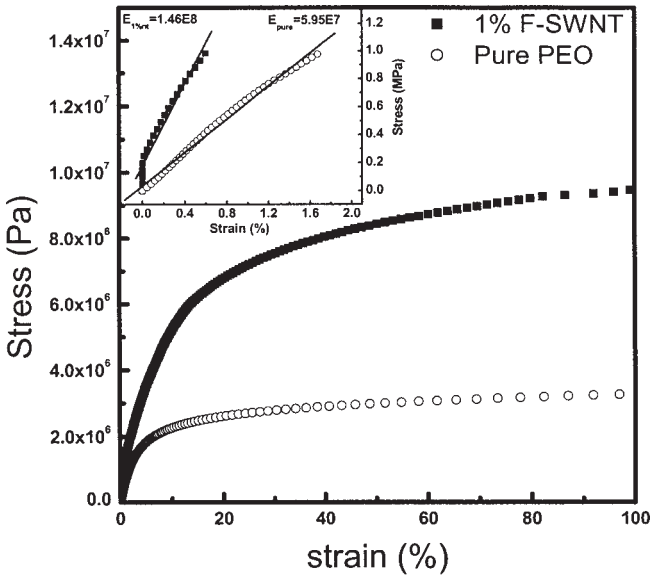

Fig. 4. The engineering tensile stress–strain curves measured at a rate of 100 mN/min. The sample with 1 wt.-% of F-SWNT has ~3× higher yield strength compared to that of the pure PEO. The elastic modulus is 5.95×10^7 and 1.47×10^8 Pa for the control sample and the PEO reinforced by 1 wt.-% of F-SWNTs, respectively.

for PEO blended with 4 wt.-% of F-SWNT. In contrast, when pristine carbon nanotubes were used without fluorination, no systematic enhancement of the mechanical properties was observed at the same nanotube loading level.

Figure 4 shows the tensile stress–strain curves of a composite with 1 wt.-% of F-SWNT and a control sample, measured at a rate of 100 mN/min. The sample with 1 wt.-% of F-SWNT has a significantly higher (~3×) yield strength compared to that of the control sample. The elastic modulus, obtained from fitting the initial slope of the stress–strain curve, is 5.95×10^7 Pa for the control sample and 1.47×10^8 Pa for the PEO reinforced with 1 wt.-% of F-SWNTs. The mechanical properties of the composites were measured in two orthogonal directions (parallel and perpendicular to the direction of the roller motion) were measured using samples from the same batch. No noticeable anisotropy was observed.

The above results show that adding a small amount of F-SWNTs drastically enhances the mechanical properties of the polymer matrix. These are in contrast to the previous studies of composites formed using pristine nanotubes where the change in the elastic properties are, in general, insignificant even at very high nanotube loading. Two recent studies reported moderate increase in the storage modulus in polymer composites blended with multi-walled carbon nanotubes (MWNTs). The RT E' was found to increase by ~60 % (from ~6 GPa to 10 GPa) when 50 wt.-% of MWNTs was added to poly(vinyl alcohol) (PVOH) matrix by solution cast.[18] A separate study reported a factor of ~2 increase in the storage modulus when 26 wt.-% of MWNTs was added to poly(methyl methacrylate) (PMMA).[19]

The large increase of the elastic modulus at low nanotube loading suggests effective load transfer from the matrix to the F-SWNTs in the current system. The results were analyzed using the equation developed for short-fiber composites:[20,21]

$$E = C_l C_o V_f E_f + (1-V_f) E_m \quad (1)$$

where E, E_f, E_m are the moduli of the composite, fiber, and polymer matrix, and C_l and C_o are coefficients related to the fiber length and orientation, respectively. For three-dimensionally randomly oriented fibers, as in the case of the F-SWNTs in PEO, C_o is about 0.2.[21,22] Using the average elastic modulus of 0.3 GPa measured for the control sample at 20 °C as the value for E_m, and assuming unity for C_l, the elastic modulus of the F-SWNT bundle is calculated to be around 0.1 TPa. The value is higher when a lower number is used for C_l. This is surprisingly close to the reported value of 1 TPa calculated[23] and the upper value derived experimentally[3] for an isolated CNT, especially when considering that defects were not taking into accounts in the calculation. In addition, SWNT bundles with weak van der Waals inter-tube bonding were used in the current experiments, rather than isolated SWNTs. The close agreement between elastic modulus calculated from the equation derived for short-fiber composites and the value measured from an isolated nanotube and nanotube bundles[24] indicates that there is an efficient load

  0935-9648/02/1910-1389 $ 17.50+.50/0

ADVANCED MATERIALS

transfer between the F-SWNTs and PEO matrix. In comparison, in the PVOH/CNT system, the calculated elastic modulus of the CNTs is only 150 MPa.[18] The lower value was attributed to the weak interfacial coupling. In addition, the results reported here show that side-wall fluorination does not significantly reduce the mechanical performances of the carbon nanotubes. At this point, it is not clear whether the enhanced load transfer, compared to composites using pristine CNTs, is due to chemical bonding between the fluorine and PEO or/and due to improved dispersion of the F-SWNTs in the polymer matrix and consequently increased entanglement between nanotubes and the polymeric chains.

In summary, we show that composites with improved uniformity and dispersion can be formed using chemically functionalized carbon nanotubes. A significant enhancement of the mechanical properties was obtained at low nanotube loading. In contrary to previous results from pristine nanotubes, the composites show efficient load transfer between the fillers and matrix.

Experimental

Sample Preparation: For the fluorination reaction 10–15 mg purified SWNTs were dispersed in dimethylformamide (DMF) by sonication. Filtering the solution through a Nylon filter membrane (Milipore, pore size 0.45 μm) resulted in a black film on the surface. The film was then peeled off and baked in air at 100 °C for several hours. It was fluorinated following the procedure described by Mickelson et al. [10]. First it was transferred into a Monel reactor and heated to 260 °C in flowing argon. The gas was then switched to a mixture of fluorine gas (20 %) and nitrogen (80 %) for ten hours at constant total flow rate of 30 sccm.

The Roll-Cast System: The roll-cast system comprises two opposing parallel rollers made of Teflon and stainless steel, respectively, and an electrical motor. The gap distance between the Teflon and the passive stainless steel roller, which is placed on a translational stage, can be adjusted using a micrometer to obtain the desired film thickness. F-SWNTs were first suspended in isopropanol by sonication and were then mixed with a clear PEO/methanol solution. They were dropped slowly onto the Teflon roller using a pipette while it's rotating. A solid film formed after evaporation of the solvent. The film was peeled off, folded, and cut to $0.2 \times 1 \times 7$ mm^3 samples for mechanical test. The samples are considerably more uniform than those formed using pristine CNTs. PEO (consists of repeating –O–CH_2–CH_2 units) powder with a molecular weight of 30 000 g/mol was purchased from Aldrich and used without further processing.

Received: August 30, 2001
Final version: July 11, 2002

[1] S. Iijima, *Nature* **1991**, *354*, 56.
[2] *Carbon Nanotubes: Synthesis, Structure, Properties, and Applications. Topics in Applied Physics* (Eds: M. S. Dresselhaus, G. Dresselhaus, P. Avouris), Vol. 80, Springer-Verlag, Heidelberg **2000**.
[3] E. W. Wong, P. E. Sheehan, C. M. Lieber, *Science* **1997**, *277*, 1971.
[4] P. M. Ajayan, O. Zhou, in *Carbon Nanotubes: Synthesis, Structure, Properties, and Applications. Topics in Applied Physics* (Eds: M. S. Dresselhaus, G. Dresselhaus, P. Avouris), Vol. 80, Springer-Verlag, Heidelberg **2000**, p. 289.
[5] L. S. Schadler, S. C. Giannaris, P. M. Ajayan, *Appl. Phys. Lett*. **1999**, *73*, 3842.
[6] C. Bower, R. Rosen, L. Jin, J. Han, O. Zhou, *Appl. Phys. Lett.* **1999**, *74*, 3317.
[7] R. Haggenmueller R. A. G. Rinzler, J. E. Fischer, K. I. Winey, *Chem. Phys. Lett*. **2000**, *330,* 219.
[8] L. Jin, C. Bower, O. Zhou, *Appl. Phys. Lett.* **1998**, *73*, 1197.
[9] O. Lourie, D. E. Cox, H. D. Wagner, *Phys. Rev. Lett*. **1998**, *81*, 1638.
[10] E. T. Mickelson, C. B. Huffman, A. G. Rinzler, R. E. Smalley, R. H. Hauge, J. L. Margrave, *Chem. Phys. Lett.* **1998**, *296*, 188.
[11] M. A. Hamon, J. Chen, H. Hu, Y. Chen, M. E. Itkis, A. M. Rao, P. C. Eklund, R. C. Haddon, *Adv. Mater.* **1999**, *11*, 834.
[12] E. T. Mickelson, I. W. Chiang, J. L. Zimmerman, P. J. Boul, J. Lozano, J. Liu, R. E. Smalley, R. H. Hauge, J. K. Margrave, *J. Phys. Chem. B* **1999**, *103*, 4318.
[13] A. Thess, R. Lee, P. Nikdaev, H. Dai, P. Petit, J. Robert, C. Xu, Y. H. Lee, S. G. Kim, A. G. Rinzler, D. T. Colbert, G. E. Scuseria, D. Tomanek, J. E. Fischer, R. E. Smalley, *Science* **1996**, *273*, 483.
[14] X. P. Tang, A. Kelinhammes, H. Shimoda, L. Fleming, C. Bower, S. Sinha, O. Zhou, Y. Wu, *Science* **2000** *228*, 492.
[15] O. Zhou, B. Gao, C. Bower, L. Fleming, H. Shimoda, *Mol. Cryst. Liq. Cryst.* **2000**, *340*, 541.
[16] R. J. Albalak, E. L. Thomas, *J. Polymer Sci., Part B: Polym. Phys.* **1993**, *31*, 37.
[17] M. Armand, J. Y. Sanchez, M. Gauthier, Y. Choquette, in *Electrochemistry of Novel Materials: Frontiers of Electrochemistry* (Eds: J. Lipkowski, P. N. Ross), VCH, Weinheim **1994**.
[18] E. P. Giannelis, in *Biomimetic Materials Chemistry* (Ed: S. Mann), VCH, Weinheim **1996**.
[19] F. Croce, G. B. Appetecchi, L. Persi, B. Scrosati, *Nature* **1998**, *394*, 456.
[20] M. S. P. Shaffer, A. H. Windle, *Adv. Mater.* **1999**, *11*, 937.
[21] Z. Jin, K. P. Pramoda, G. Xu, S. H. Goh, *Chem. Phys. Lett.* **2001**, *337*, 43.
[22] H. Fukuda, K. Kawata, *Fibre Sci. Technol.* **1974**, *7*, 207.
[23] T. W. Chou, *Microstructural Design of Fiber Composite*, Cambridge University Press, Cambridge **1992**.
[24] J. W. D. Callister, *Materials Science and Engineering: An Introduction*, 3rd ed., Wiley, New York **1994**.
[25] J. P. Lu, *Phys. Rev. Lett*. **1997**, *79*, 1297.
[26] J. P. Salvetat, G. Andrew, D. Briggs, J. M. Bonard, R. R. Bacsa, A. J. Kulik, T. Stockli, N. A. Burnham, L. Forro, *Phys. Rev. Lett*. **1999**, *82*, 944.

Selective Fabrication of Carbon Nanocapsules and Mesocellular Foams by Surface-Modified Colloidal Silica Templating**

By *Jyongsik Jang** and *Byungkwon Lim*

The diverse applicability of nanometer-sized carbon materials has motivated the development of various methods of fabricating tailored carbon nanostructures, such as nanotubes, hollow capsules, and mesoporous forms.[1] In particular, mesoporous carbon provides a controlled pore size and high surface area, and can be applied to nanoreactors, catalysts, adsorbents, optical devices, and electrochemical supercapacitors.[2] On the other hand, hollow carbon nanostructures are useful for the purposes of drug delivery, the protection of proteins and enzymes, and as sensors and storage materials.[3]

Recently, various porous and hollow carbon nanostructures have been prepared by templating procedures. Porous carbon nanostructures have been synthesized by using zeolites, mesoporous silicas,[4] and opals[5] as the templates. The fabrication of porous carbon using porous silica templates generally involves filling the pores with a carbon precursor, followed by carbonization and the subsequent removal of the template. Hollow carbon nanostructures have also been obtained using submicrometer-sized polymeric[6] and inorganic[7] spheres as the template, by forming a template-carbon core–shell parti-

[*] Prof. J. Jang, B. Lim
School of Chemical Engineering and Hyperstructured Organic Materials Research Center, Seoul National University
Seoul 151-742 (Korea)
E-mail: jsjang@plaza.snu.ac.kr

[**] This work was supported by the Brain Korea 21 program of the Korean Ministry of Education and Korea Science and Engineering Foundation through the Hyperstructured Organic Materials Research Center.

  0935-9648/02/1910-1390 $ 17.50+.50/0